Extraction and Synchronization of BOLD Spontaneous Oscillations using Singular Spectrum Analysis

Danilo Menicucci,
Angelo Gemignani,
Andrea Piarulli,
Remo Bedini

*Extreme Centre,
Scuola Superiore
Sant'Anna - CNR,
Pisa, Italy*

Claudio Gentili,
Giacomo Handjaras,
Sabrina Danti,
Mario Guazzelli

*Department of Psychiatry,
Neurobiology,
Pharmacology and
Biotechnology,
University of Pisa, Italy*

Marco Laurino
Paolo Piaggi,
Alberto Landi

*Dep. of Electrical Systems
and Automation,
University of Pisa, Italy*
landi@dsea.unipi.it

Abstract

Spontaneous cerebral blood oxygenation level-dependent (BOLD) fluctuations are gaining interest in the neurophysiology community. These oscillations are prominent in the low-frequency range with spatiotemporal correlations. From a healthy individual, a basal resting state BOLD fMRI acquisition has been performed by collecting 4 slices. Voxel signals from seven selected regions have been considered. We assumed a composite null-hypothesis of oscillations embedded in "red noise". To extract oscillations from BOLD signals we applied the Monte Carlo Singular Spectrum Analysis (SSA). Phase-synchronization of the oscillatory components, in the low-frequency range 0.085-0.13Hz, have been also achieved. As results, region-dependent distributions were apparent both for the noise parameters and for the number of connections between voxels. Although further studies on population samples should confirm the result consistency, the SSA technique combined with a phase-synchronization analysis seems a feasible method to extract low frequency BOLD spontaneous oscillations and to find functional connections among cerebral areas.

1. Introduction

In the last decade, functional magnetic resonance imaging (fMRI) was used to assess brain correlates of mind functions. The physical base of this method is related to the magnetic properties of deoxy- and oxyhemoglobin which give a different BOLD (blood oxygen level dependent) signal magnitude. Neural and vascular activities are in fact coupled together and thus it is possible to study neural activations through vascular activity. However several specific aspects of the BOLD signal are still unclear. Among these:

Which are the neurophysiologic meanings of the spontaneous BOLD signal oscillations?

Does BOLD signal have features that are specific for each individual or for each type of brain tissue (i.e. white matter, grey matter, etc)?

Solving these questions will lead to a better understanding of brain functioning. For these reasons, recently resting brain networks have begun to be explored with several methodologies [1], [2].

For example Cordes and co-workers in 2001 [3] identified specific spectrum components of the BOLD signal related to heartbeat, respiration, neurovascular coupling and vasomotion. Particular interest attains the two latter phenomena and it can be suggested that slow oscillations in BOLD signals could be inherent to action of local feedbacks on the control of parameters such as blood flow or gasses concentration.

Our study aimed at identifying time-varying BOLD oscillatory components and at studying the coupling between voxels (within and between cerebral areas), namely we measured the temporal correlation between two neuropsychological events that are spatially distant (functional connectivity [4]). To these aim, a SSA (Singular Spectrum Analysis) based approach is proposed.

978-0-7695-3872-3/09 $26.00 © 2009 IEEE
DOI 10.1109/ISDA.2009.178

IEEE computer society

2. Methods

2.1. fMRI data acquisition

We used a 1.5 Tesla GE scanner (General Electric, Milwaukee, WI) to acquire basal resting state data for about 10 mins (1970 time points) from one healthy volunteer with a GR-EPI sequence (FOV 24; TR/TE= 300/40 msec; FA=90°; resolution = 64×64 pixels; voxel size 3,75x3,75x5 mm, REPS=2000) to collect 4 slices aligned to the commissural line. To test the feasibility of the sequence parameters to detect the BOLD signal we performed several ad-hoc scan sessions with a simple motor task (finger tapping) with different TR (2000, 500, 300 and 100 msec) and same FA, TE and resolution. We did not find any significant differenceses in signal change during the task across different TR conditions. In addition the maximum displacement of subject head during the scan session was below 0.7 mm, therefore, the movement correction has not been taken into account.

SSA was performed on selected voxels from different regions of the brain (Figure 1). Starting from the regions we acquired with the EPI sequence, we drawn Regions of Interest (ROI) of grey matter according to available litterature suggesting a role in different resting state functional networks [5]. We choose middle prefrontal cortex (MPFC) and insula (default mode network), dorsolateral prefrontal cortex (DLPFC) (dorsal attentional network), superior temporal sulcus (STS), cuneus (ventral attentional network), white matter (anterior part of the semioval center), lateral ventricles on a high-resolution T1-weighted spoiled gradient recall images (1.2-mmthick axial slices; TR = 12.1ms; TE = 5.22 ms; FA = 20◦; FOV= 24 cm; resolution = 256×256 pixels).

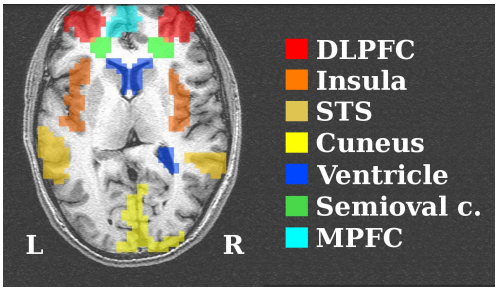

Figure 1. fMRI ROI (overlapped slices)

2.2 Singular Spectrum Analysis

The Singular Spectrum Analysis (SSA) is a novel technique for time series decomposition. It decomposes a time series $d(t)$ to obtain a set of distinct uncorrelated components ($\boldsymbol{R}(t)$, trends and oscillatory components) and structureless noise $\varepsilon(t)$ [6], [7] and [8]:

$$d(t) = \sum_k R_k(t) + \varepsilon(t)\,. \tag{1}$$

SSA is nonparametric and its decomposition is based on a data-adaptive basis set, instead of the usual sinusoidal one. SSA operates in these steps.

Embedding step.

A trajectory matrix D is derived from $d(t)$ (length N). The i-th column of D contains a portion of $d(t)$ from $d(i)$ to $d(i+w-1)$.
The window length w can be set from 2 to $N/2$.
The number of the columns of $\boldsymbol{D}$ is: $M=N-w+1$.
From the $\boldsymbol{D}$, a $w \cdot w$ lag-covariance matrix $\boldsymbol{C_D}=\eta \boldsymbol{D^T D}$ where $\eta=1/(N-w+1)$ accordingly to Broomhead and King method (suitable for non stationary signal [10]) is derived [9].

SVD step.
$\boldsymbol{C_D}$ is diagonalized as

$$\Lambda_D = E_D^T C_D E_D \tag{2}$$

where $\boldsymbol{\Lambda_D}$ is the eigenvalue ordered (decreasing order) diagonal matrix and $\boldsymbol{E_D}$ is the matrix of eigenvectors or Empirical Orthogonal Functions (EOFs). Each EOFs has an associated dominant frequency (DF).

Monte Carlo SSA step.

The signal/noise separation is performed under weaker conditions than the classical truncation procedure [11]. It can be assumed that $d(t)$ is composed by oscillations with different frequencies embedded in the noise.

Also the noise model has to be specified: we considered a first order autoregressive (AR(1)) model of noise, also named "red" or "Brownian" noise. Red noise because its power spectrum is biased towards low frequencies, although it doesn't present harmonic oscillatory modes.

More, the AR(1) model also inherits the case of uncorrelated ("white") noise. The recursive equation that describe the red noise model is:

$$u_t - u_0 = \gamma\left(u_{t-1} - u_0\right) + \alpha z_t\,, \tag{3}$$

where u_0 is the process mean, γ and α are process parameters and z_t is a Gaussian, unit-variance white noise.

In the case of $\gamma = 0$ the model downgrades to a white noise model.

The estimation of the red noise parameters γ and α from the $d(t)$ is performed by a maximum-likelihood criterion [12], [13]. These estimators nearly unbiased also for short series $d(t)$, the condition is $N \sim -10 \cdot 1/\log(\gamma)$ or greater.

From the estimated noise model, it derives the analytic noise covariance matrix $\boldsymbol{C_N}=c_0\boldsymbol{W}$, where c_0 is the noise variance and $\boldsymbol{W_{ij}}=\gamma^{|i-j|}$.

The expected EOFs of the noise are obtained by diagonalizing $\boldsymbol{C_N}$ as:

$$\Lambda_N = E_N^T C_N E_N \,. \tag{4}$$

Under the assumptions of Gaussian noise distribution and sinusoidal EOFs, each diagonal element of $\boldsymbol{\Lambda_N}$ (λ_N) has a chi-squared distribution with $\upsilon=3N/w$ degrees of freedom. These assumptions are valid for AR(1) processes [14] as

$$\lambda_N \approx \varepsilon(\lambda_N)\chi^2(\nu)/\nu \,, \tag{5}$$

where $\varepsilon(\lambda_N) = \left(E_N^T C_N E_N\right)_{kk}$ and ε is the expectation operator.

From the 2.5th and 97.5th percentiles of these distributions, for each λ_N a confidence interval can be derived. Then, the data covariance matrix $\boldsymbol{C_D}$ is projected onto noise EOFs:

$$\Lambda'_D = E_N^T C_D E_N \,. \tag{6}$$

In the null-hypothesis of pure red noise model generating $d(t)$, all diagonal elements of $\boldsymbol{\Lambda'_D}$ (λ'_D) should lie within the noise confidence interval of the λ_N with the same DF.

Otherwise, EOFs associated with λ'_D lying outside the corresponding confidence interval are considered not compatible with the noise model, and thus they indicate presence of oscillators embedded in the noise at that frequency.

It's worth noting that eigenvalues can be outside confidence intervals both in the upper and in the lower side. Experimenters, on the basis of phenomena knowledge, should choose between the selection of EOFs with greater or smaller λ'_D compared to noise eigenvalue spectrum.

Figure 2 shows an example of application of Monte Carlo SSA procedure considering a cuneus voxel. The resulting projection λ'_D of data covariance matrix $\boldsymbol{C_D}$ onto the expected EOFs of the noise $\boldsymbol{E_N}$ is computed and error-bars are drawn from confidence intervals of each λ_N.

$\boldsymbol{E_N}$ dominant frequency are regularly spaced, separated by $\sim 1/(w \cdot T_c)$ where T_c =0,3 sec.

We consider significant all λ'D lying above the 97.5th percentile of their corresponding error-bars.

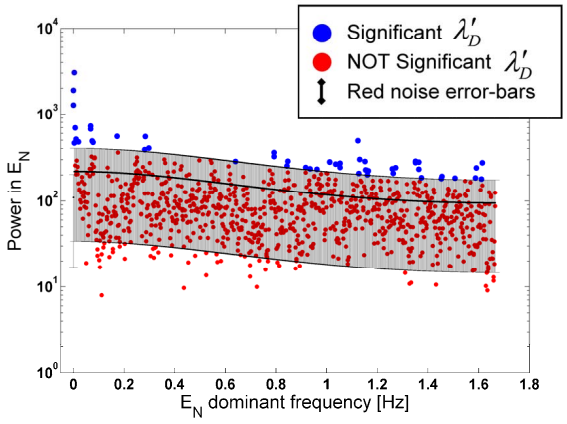

Figure 2. Monte Carlo SSA on a cuneus voxel

We name E_N^S the matrix extracted from $\boldsymbol{E_N}$ composed by EOFs associated with selected λ'_D. In order to identify significant data EOFs, for each EOF in E_N^S, the cross-correlations with $\boldsymbol{E_D}$ is computed and the maximally correlated EOF from $\boldsymbol{E_D}$ is extracted.

We name E_D^S the matrix composed by the selected data EOFs.

Reconstruction step.

The projection of $d(t)$ onto each k-th significant data EOFs yields the corresponding significant principal components $\boldsymbol{A_k}$ [15]

$$A_k(t) = \sum_{j=1}^{w} d(t+j-1)E_k^S(j) \tag{7}$$

where $E_k^S(j)$ identifies the j-th element in the k-th column of E_D^S.

For each EOF in E_D^S, the corresponding reconstructed component Rk(t) is obtained by the convolution:

$$R_k(t) = \frac{1}{M_t}\sum_{j=L_t}^{U_i} A_k(t-j+1)E_k^S(j) \tag{8}$$

where Mt, Lt and U_t are time-index t dependent factors,

necessary to manage border effects [16].

Actually, in the case of oscillatory modes embedded in the noise, SSA identifies, for each of them, a pair of EOFs, and thus of $R_k(t)$. Namely, for each mode two nearly equal eigenvalues, associated to EOFs with the same DF and $\pi/4$ out of phase with each other are expected.

At variance, the two reconstructed components $R_k(t)$, by means of the convolution precedure, do not show the $\pi/4$ phase delay. Finally, each oscillatory mode is obtained summing up the paired $R_k(t)$.

2.3. Dominant frequency estimation

Extracted EOFs and components are nearly "monochromatic", thus a low order all-pole model can be used for the DF estimation.

A forth-order AR model has been estimated by the Burg method [17].

Two cases occurred: 1) components showed a pair of poles at 0 Hz; 2) a pair of poles with associated more than 95% of the variance explained by the model.

In the first case, the DF is the frequency of the remaining pair of poles, in the latter case the DF is the frequency of the dominant pair of poles.

2.4. Phase synchronization

Entrainment between voxels has been evaluated.

For each pair of voxels, all pairs of components composed by a component of one voxel with a component of the other voxel have been collected.

For each voxel, phase synchronization between each component pair has been estimated. Pairs of voxels with, at least, one component pair significantly synchronized has been considered coupled. Concerning the phase synchronization, instantaneous phases of each component was derived by Hilbert transform [18].

Given the phase series Φ_i and Φ_j, the phase synchronization index, $PSI(t_n)$ between the components i and j was estimated as follows [19], [20]:

$$PSI(t_n) = \sqrt{C_{ij}(t_n)^2 + S_{ij}(t_n)^2} \tag{9}$$

$$S_{ij}(t_n) = \frac{1}{w/\Delta t} \sum_{m=-w/2\Delta t}^{m=w/2\Delta t} \sin\left[\phi_i(t_n + m\Delta t) - \phi_j(t_n + m\Delta t)\right] \tag{10}$$

$$C_{ij}(t_n) = \frac{1}{w/\Delta t} \sum_{m=-w/2\Delta t}^{m=w/2\Delta t} \cos\left[\phi_i(t_n + m\Delta t) - \phi_j(t_n + m\Delta t)\right] \tag{11}$$

where w (here set to $5/DF$) is the time window used to calculate PSI and t_n is the time center of the window (here we moved the window with a $1/(2 \cdot DF)$ step).

The PSI ranges from 0 to 1 and high values indicate a phase coupling between signals. In order to fix significance threshold on PSI values related to real entrainment, a surrogate-based method [21] was used.

Effectively, for each pair of components, the PSI was estimated matching the phase of signal i in the time window centered at t_1 with the phase of signal j in the time window centered at a different time t_2, randomly drawn. Repeating this procedure one hundred times for each t_1, a huge distribution of the by *chance-PSI* values was estimated. The 95-th percentile of this distribution was used as threshold.

PSI values exceeding this threshold were considered indicating a real phase entrainment.

3. Analysis of BOLD signals

The present work shows an application of the SSA on cerebral signals, in details:

- fMRI BOLD signals were analyzed by the SSA technique. We model BOLD signals as oscillatory components embedded in "red noise". For each time series, it has been extracted:
  - an estimation of the lag-1 autocorrelation of the red noise, γ
  - a set of reconstructed components $R_k(t)$ related to embedded oscillatory modes.
- Extracted oscillatory components have beenclassified with a DF-based criterion. They were clustered by a k-means approach. Using the Krzanowski-Lai sum-of-squares criterion, the optimal number of groups has been set [22].
- Trends, respiratory- and cardiac-related components have been discarded.
- Synchronization between retained oscillatory components of different voxels has been studied. Synchronization was evaluated for each pair of voxels. A pair of voxels was considered linked if, at least, one pair of components (one component from the first voxel with one component from the second voxel) was significantly phase coupled.

Concerning the SSA application, in order to obtain the maximal spectral resolution of the reconstructed components and to detect slow periodic oscillations on BOLD signals, we choose w = 985 time points (equal to half of the time series length, N=1970).

4. Results

The application of SSA on BOLD signals identified, on average, 12±4 oscillatory modes from the signal of each voxel. From the red noise model estimation, the lag-1 autocorrelation (γ) was estimated for each voxel.

Figure 3 shows the map of γ rendered onto highresolution anatomical scans. Areas with, on average, high γ compared to the general mean can be identified. Both the cuneus and the superior temporal sulcus regions, bilaterally in this subject had significant higher mean γ.

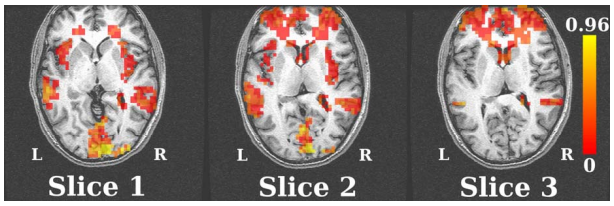

Figure 3. Map of γ rendered onto anatomical scans

Extracted components were clustered in 4 groups by the k-means approach. Clustering identifies well-separated groups of frequencies: a cardiac one (0.8-1.2 Hz), a respiratory one (0.15-0.4 Hz) a low frequency one (LF, 0.085-0.13 Hz) and a nearly trend one (0-0.085 Hz).

The analysis of synchronization was focused on the oscillatory modes in the LF group, since superimposed on the vasomotion frequency band. As first results, we counted the number of links in which each voxel was involved.

We separate the counting considering 4 cases:

1) Links to voxels in the same region (and hemisphere).
2) Links to voxels in the contralateral region.
3) Links to voxels in different regions but in the same hemisphere.
4) Links to voxels in different regions (excluded the contralateral region) of the contralater hemisphere.

For each case, the amount of links per voxel was normalized to the maximal number of possible links in that case. Interestingly, some region-dependent distributions of connections were apparent: this holds in particular for cases (1) and (3).

Figure 4 shows the map of connections in the case (1) rendered onto high-resolution anatomical scans. The most wired regions, the cuneus regions bilaterally exhibit the higher values of intra-region connections.

Figure 5 shows the map of connections in the case (3) rendered onto high-resolution anatomical scans. Regions in left hemisphere (the dominant one) exhibited higher number of connections.

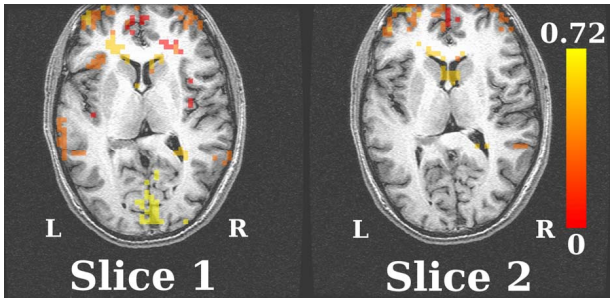

Figure 4. Map of intra-region connections in the vasomotion frequency band (case 1)

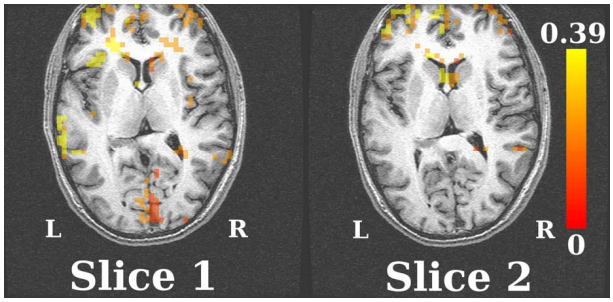

Figure 5. Map of intra-hemisphere connections in the vasomotion frequency band (case 3)

5. Conclusions

The SSA along with a phase synchronization analysis resulted a feasible method to analyze low-frequency BOLD spontaneous oscillations.

In fact, its applicability to non-stationary processes and phase- and amplitude-modulated oscillations makes it suitable for the BOLD signals analysis and may lead to the detection of hidden non-constant BOLD fluctuations.

In addition, the Monte Carlo SSA algorithm based on the composite null hypothesis of signal plus AR(1) noise makes unnecessary any pre-processing of the data (removing of trend or artifactual periodic components such as cardiac or respiratory oscillations).

The red noise was chosen to describe the biological noise in the fMRI based signals: this choice introduced a more stringent null-hypothesis to test for oscillations at low frequencies compared to white noise modeling.

As main descriptive results of this preliminary study we showed some region-dependences of the red-noise parameters and of the synchronization in the LF band.

Further studies conducted on population samples would clarify the consistency and the possible neurophysiologic correlates of these differential distributions.

6. References

[1] D.P. Auer, "Spontaneous low-frequency blood oxygenation level-dependent fluctuations and functional connectivity analysis of the 'resting' brain," *Magnetic Resonance Imaging*, 2008.

[2] M.D. Fox *et al*., "Intrinsic fluctuations within cortical systems account for intertrial variability in human behavior," *Neuron*, 2007.

[3] D. Cordes et al., "Frequencies contributing to functional connectivity in the cerebral cortex in "resting-state" data," *American Journal of Neuroradiology*. 2001.

[4] K.J. Friston, "Functional and effective connectivity in neuroimaging: A synthesis," *Hum Brain Mapping,* 1994.

[5] M. D. Fox and M. E. Raichle, "Spontaneous fluctuations in brain activity observed with functional magnetic resonance imaging," *Nat Rev Neurosci*, 2007.

[6] N. Golyandina, V. Nekrutkin, and A. Zhigljavsky, *Analysis of Time Series Structure: SSA and Related Techniques*, Chapman & Hall/CRC, New York, 2001.

[7] M. Ghil , *et al*., "Advanced spectral methods for climatic time series," *Rev. Geophys*., 2002.

[8] J.B. Elsner, and A.A. Tsonis, *Singular Spectrum Analysis*, Plenum, New York, 1996.

[9] D.S. Broomhead, and G.P. King, "Extracting qualitative dynamics from experimental data," *Physica D*, 1986a.

[10] R. Vautard, and M.Ghil, "Singular spectrum analysis in nonlinear dynamics, with applications to paleoclimatic time series," *Physica D*, 1989.

[11] H.F. Kaiser, "The varimax criterion for analytic rotation in factor analysis," *Psychometrica*, 1958.

[12] M.R. Allen, P.L. Read and L.A. Smith, "Temperature time-series?," *Nature*, 1992a.

[13] M.R. Allen, P.L. Read and L.A. Smith, "Temperature oscillations," *Nature*, 1992b.

[14] M.R. Allen, and L.A. Smith, "Monte Carlo SSA: Detecting irregular oscillations in the presence of coloured noise," *Journal of Climate*, 1996.

[15] I. T. Jolliffe, *Principal Component Analysis*, Springer-Verlag, New York, 2002.

[16] M.Ghil , and R. Vautard, "Interdecadal oscillations and the warming trend in global temperature time series," *Nature*, 1991.

[17] J. P.Burg, "Maximum entropy spectral analysis," *37th Annual Meeting, Society of Exploration Physicists*, Oklahoma City, OK, 1967.

[18] L. Cohen, *Time-Frequency Analysis*, Prentice Hall,1995.

[19] M. Rosenblum, *et al*., "Phase synchronization: from theory to data analysis," *Neuro-informatics and neural modelling*, 2000.

[20] J. Ito, AR Nikolaev, and C. van Leeuwen, "Spatial and temporal structure of phase synchronization of spontaneous alpha EEG activity," *Biol Cybern*., 2005

[21] T. Schreiber, and A. Schmitz. "Surrogate time series," *Physica D*, 2000.

[22] W.J. Krzanowski, and Y.T. Lai, "A criterion for determining the number of groups in a data set using sum-of-squares clustering," *Biometrics*, 1988.